

Design for the Detection of the Singly-Connected Superconducting State

Jorge Berger^o and Jacob Rubinstein^{*}

^oDepartment of Physics, Technion, 32000 Haifa, Israel

^{*}Department of Mathematics, Technion, 32000 Haifa, Israel

We study the Little-Parks effect for mesoscopic loops with very nonuniform thickness. The results follow the trend of the phase diagram obtained for almost uniform thickness. In particular, the singly-connected state is stable on a line segment delimited by two critical points. Most of this study considers loops with piecewise constant thickness; in this case the Euler-Lagrange equation can be integrated analytically. Under appropriate conditions, the temperature range where the singly-connected state is stable is proportional to the square of the ratio between the maximal and the minimal thicknesses. Our results may serve as a guide for planning experiments.

PACS numbers: 74.60.Ec

I. INTRODUCTION

We deal with a loop of superconducting material as shown in Fig. 1. If the entire loop is superconducting and if it encloses a non-integer number of magnetic flux quanta, then single-valuedness of the order parameter requires the presence of some supercurrent I . This supercurrent involves an energy price and, due to it, the transition to superconductivity occurs at lower temperatures when the enclosed flux is non-integer. This effect was observed by Little and Parks¹ and an explanation in terms of the Ginzburg-Landau theory was provided by Tinkham.²

We have recently predicted that, if the thickness of the loop is not exactly uniform, then there exist situations for which superconductivity is broken at a layer, so that the superconducting part is actually singly-connected³ and no supercurrent flows. When this happens, we say that the sample is in the “singly-connected state” (SC). This is an interesting possibility, since it would allow for a new dimensionality of the regions where the order parameter may vanish. In the case of vortices, the order parameter vanishes along lines and there are claims⁴ that it cannot vanish on surfaces. On the other hand, it has been suggested that even for uniform thickness the SC state will appear as an intermediate station in hysteretic paths.⁵ A systematic analytic study for the stability domain of the SC state in families of loops with thicknesses that deviate slightly from uniformity was carried on in Ref. 6. Mathematical justification for some of the assumptions in our model is given in Ref. 7. Another situation in which the order parameter seems to vanish on a layer was considered in Refs. 8 – 9.

Since Ref. 6 may be too mathematically oriented, we shall review here its central findings. We assume that the thickness of the loop (radial dimension) is much smaller than the perimeter. In this case, for the range of temperatures at which transitions occur, the order parameter is uniform on cross sections of the loop. (A “cross section” is a surface which is everywhere normal to the supercurrent.) In addition, the free energy is insensitive to the magnetic field created by I and to the linear shape of

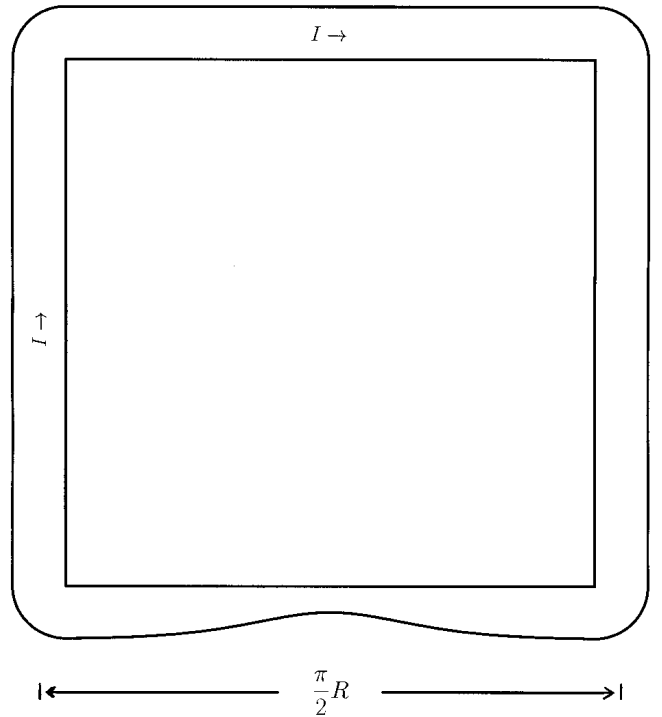


FIG. 1. Thin loop of superconducting material with perimeter $2\pi R$ and nonuniform cross section D . The magnetic flux enclosed by the loop is Φ and the supercurrent around it is I .

the loop. We may therefore regard the loop as a circular ring with radius R equal to the perimeter divided by 2π . We define by θ the angle which is obtained by deforming the loop to a circle, i.e. θ is the arc length divided by R ; the “thickness” $D(\theta)$ is defined as the area of the cross section at θ . The origin $\theta = 0$ is defined by requiring that

$$\int_0^{2\pi} D(\theta) \sin \theta d\theta = 0 \quad (1)$$

and

$$\beta = 2 \int_0^{2\pi} D(\theta) \cos \theta d\theta / \int_0^{2\pi} D(\theta) d\theta < 0 \quad (2)$$

The controllable physical coordinates are the temperature T and the magnetic flux Φ . They enter our equations through

$$\lambda = \frac{R^2}{\xi^2} = \frac{T_c - T}{T_c - T_R} \quad (3)$$

and

$$k = n - \Phi/\Phi_0, \quad (4)$$

where ξ is the coherence length, T_c is the critical temperature in the absence of magnetic field, T_R is the temperature at which $\xi = R$, Φ_0 is the quantum of magnetic flux and n is some integer.

Let $\psi(\theta)$ be the order parameter and ψ_0 the order parameter that would be obtained in the absence of magnetic field. We define $y(\theta) = |\psi(\theta)/\psi_0|$. The contribution of superconductivity to the free energy is proportional to

$$\int_0^{2\pi} (-\lambda y^2 + \frac{1}{2}\lambda y^4 + (y')^2) D d\theta + (2\pi k)^2 \Lambda^{-1}, \quad (5)$$

where the prime denotes differentiation with respect to θ and

$$\Lambda = \int_0^{2\pi} \frac{d\theta}{D y^2} \quad (6)$$

is a nonlocal term. (Some symbols, such as Λ and λ_i are defined here not exactly as in Ref. 6.) The term k/Λ (cf. (5)) is proportional to the supercurrent I . Since (5) increases monotonically with k^2 , the minimum of the free energy will always occur for k in the range $[-\frac{1}{2}, \frac{1}{2}]$. Note that only the absolute value of $\psi(\theta)$ enters the expression for the the free energy; $\arg[\psi(\theta)]$ has been already worked out.

A necessary condition for a minimum of the free energy is the Euler-Lagrange (EL) equation. For the SC state $y(0) = 0$ and the EL equation is

$$(Dy')' + \lambda D(y - y^3) = 0. \quad (7)$$

When $y(\theta)$ is positive everywhere, we say that the sample is in the ‘‘doubly-connected state’’ (DC). In this case a better description is given in terms of $w = y^2$ and the EL equation reads

$$Dww'' + D'ww' - \frac{D}{2}(w')^2 + 2\lambda Dw^2(1 - w) - \frac{2}{D} \left(\frac{2\pi k}{\Lambda} \right)^2 = 0. \quad (8)$$

The phase diagram in the temperature - magnetic field plane is shown in Fig. 2. N, DC and SC denote the three possible states and Γ_I , Γ_{II} and Γ_{III} are critical lines at which second order phase transitions occur. When Γ_{III} is approached from below, $y(0)$ decreases until it finally vanishes. Since Γ_{III} is located along $|k| = \frac{1}{2}$, and the

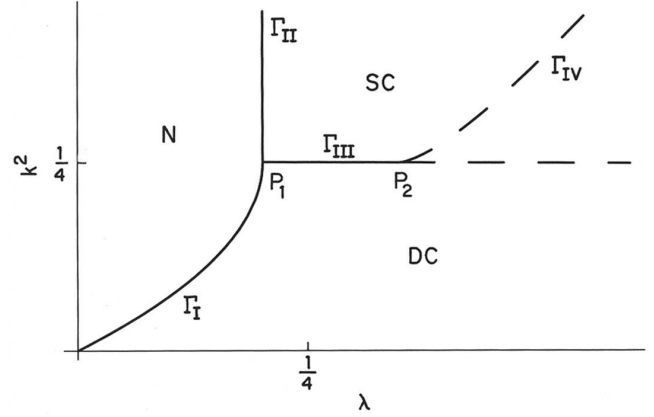


FIG. 2. Phase diagram. N: $y \equiv 0$; DC: $y > 0$ everywhere; SC: the order parameter vanishes at some place in the loop and becomes singly connected. P_1 and P_2 are critical points. λ decreases with temperature and k^2 increases with the deviation from an integer number of flux quanta.

most stable state is never at $|k| > \frac{1}{2}$, the SC stability domain is restricted to a line segment. The ends of this segment are the critical points P_1 and P_2 . When the magnetic field is varied and the line $|k| = \frac{1}{2}$ is crossed for small λ (between P_1 and P_2), the current I vanishes and changes sign continuously. However, for large λ (beyond P_2), the current I changes sign discontinuously.

Let us denote the positions of $P_{1,2}$ by $(\lambda = \lambda_{1,2}, |k| = \frac{1}{2})$. λ_1 is given by the smallest value λ for which the linearized Eq. (7) (without y^3) has nontrivial solutions. To locate λ_2 we define

$$f(\theta) = D(\theta)w(\theta), \quad \tilde{f}(\theta) = f(0) + \frac{1}{2}f''(0)\theta^2, \quad (9)$$

$$\Lambda_R = -2 \int_{\pi}^{\infty} \frac{d\theta}{\tilde{f}} + 2 \int_0^{\pi} \frac{\tilde{f} - f}{f\tilde{f}} d\theta. \quad (10)$$

Then, along Γ_{III} , Λ_R is negative (resp. zero, positive) when the value of λ is less (resp. equal, larger) than λ_2 . If $D(\theta)$ is close to uniform, then, to first order in the deviation from uniformity,

$$\lambda_1 = \frac{1}{4}(1 + \beta); \quad \lambda_2 = \frac{1}{4}(1 - 2\beta). \quad (11)$$

The analysis of Ref. 6 has an obvious shortcoming for experimental purposes: one would like the SC state to exist in a temperature range which is not too small, i.e. P_1 and P_2 are not too close. This occurs when $|\beta|$ is not too small. But most of the results reviewed above were obtained under the assumption that $D(\theta)$ is almost uniform, which implies $|\beta| \ll 1$. The purpose of this article is to study forms of $D(\theta)$ which are strongly nonuniform, to check whether the scenario depicted in Fig. 2 is still valid and whether only the first harmonic of $D(\theta)$ affects the phase diagram [since $D(\theta)$ enters Eq. (11) only through β].

In most of this article (Secs. II and III) we study the case in which $D(\theta)$ is a piecewise constant function. In this case Eq. (8) can be solved analytically. Sec. III considers the experimentally interesting limit of a weak link. We shall see that in this case P_2 can move to temperatures where superconductivity is already well developed, provided that the ratio between the length and the width of the weak link is carefully tuned. In Sec. IV we consider deviations from the piecewise constant shape and Sec. V provides suggestions for experiments which, besides the appropriate form for $D(\theta)$, are quite standard.

II. PIECEWISE CONSTANT THICKNESS

A piecewise constant thickness will be described by $D(\theta)$ of the form

$$D = \begin{cases} d & \theta < \theta^* \\ 1 & \theta^* < \theta < \pi \end{cases} \quad (12)$$

with $0 < d < 1$ and $0 < \theta^* < \pi$ constants, and $D(\theta)$ symmetric about $\theta = 0$ and about $\theta = \pi$. We are free to set the maximum of $D(\theta)$ as 1, since the EL equation is invariant under multiplication of $D(\theta)$ by a constant; d is the ratio between the minimum and the maximum thicknesses.

In this case we have found a solution of Eq. (8) with the appropriate symmetry. For $\theta < \theta^*$ we require the order parameter to have a minimum at $\theta = 0$. It has the form

$$w(\theta) = A_1 - \frac{2\nu_1^2}{\lambda} m_1 \text{cn}^2(\nu_1 \theta, m_1). \quad (13)$$

For $\theta > \theta^*$ we require a maximum at $\theta = \pi$ and the solution is

$$w(\theta) = A_2 - \frac{2\nu_2^2}{\lambda} m_2 (1 - m_2) \text{sd}^2(\nu_2 \theta, m_2). \quad (14)$$

In these expressions cn and sd are Jacobian elliptic functions,¹⁰ ν_i and m_i are constants, and

$$A_i = \frac{2}{3} \left(1 + (2m_i - 1) \frac{\nu_i^2}{\lambda} \right). \quad (15)$$

With these forms, the constant term in Eq. (8) becomes

$$\left(\frac{2\pi k}{D\Lambda} \right)^2 = \frac{A_i}{8\lambda} (\lambda^2 (A_i - 2)^2 - 4\nu_i^4). \quad (16)$$

A. Mathematical Details

Eqs. (13)–(16) reduce the integro-differential equation (8) to the problem of determining the four constants ν_i and m_i . We are thus left with four algebraic equations:

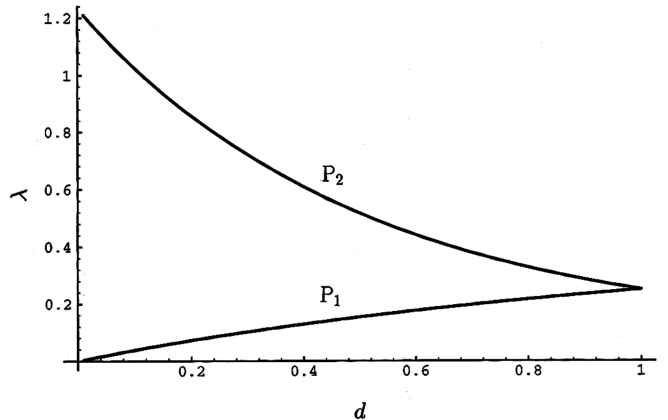


FIG. 3. Position of the critical points as functions of the ratio $d = D(0)/D(\pi)$ in (12). Here $\theta^* = \pi/2$.

Eq. (16) for $i = 1, 2$ and continuity of w and Dw' at $\theta = \theta^*$.⁶ These equations are solved by Newton iterations. The integration in (6) is performed numerically.

When $w(0) = 0$, Λ diverges and Eqs. (16) simplify to $\lambda(2 - A_i) = 2\nu_i^2$. Still for $w(0) = 0$, the numerator and the denominator of the integrand in (10) vanish for $\theta \rightarrow 0$. In this region, we expanded the integrand (analytically) into a power series.

It is sometimes useful to regard $w(0)$ as an independent variable (and k as dependent). For $0 < w(0) < 1$, the integration in (6) cannot be performed numerically near $\theta = 0$. In this region, we substitute the integrand by a Padé approximant in powers of θ^2 , with the denominator linear in θ^2 .

As Γ_1 is approached, $m_{1,2} \rightarrow 0$, and we recover the situation in subsection 4.3 of Ref. 6. As λ is increased away from Γ_1 , m_1 and m_2 increase, but m_1 increases faster than m_2 . Not far from Γ_1 , $m_1 = 1$. If λ is increased further, m_1 and ν_1 become complex numbers, with $|m_1| = 1$ and $\arg(\nu_1) = -\frac{1}{4} \arg(m_1)$. Both regimes (m_1 and ν_1 real or complex) can be unified by writing $m_1 = e^{-4t}$ and $\nu_1 = re^t$: Eqs. (13) and (15) together with relationships 16.9.1 and 16.11.3 of Ref. 10 show that w is an even function of t . It follows that $w(\theta)$ depends on t only through t^2 ; more precisely, $w(\theta)$ is an analytic function of t^2 which is real when t^2 is real, and nothing special happens when t^2 changes sign. This means that w is still real when m_1 and ν_1 become complex, and there is no singularity at $m_1 = 1$. Our computer programs used different parametrizations for the cases $0 < m_1 < 1$ and $|m_1| = 1$. Since we are mostly interested in the region where λ is large, in some cases we did not perform calculations in the region where $0 < m_1 < 1$.

B. Dependence of $\lambda_{1,2}$ on d

By a straightforward generalization of subsection 4.3 in Ref. 6, we obtain

$$d = \tan(\sqrt{\lambda_1}(\pi - \theta^*)) \tan(\sqrt{\lambda_1}\theta^*). \quad (17)$$

λ_1 is obtained by solving this equation. λ_2 is obtained by solving numerically $\Lambda_R = 0$ for the situation $w(0) = 0$.

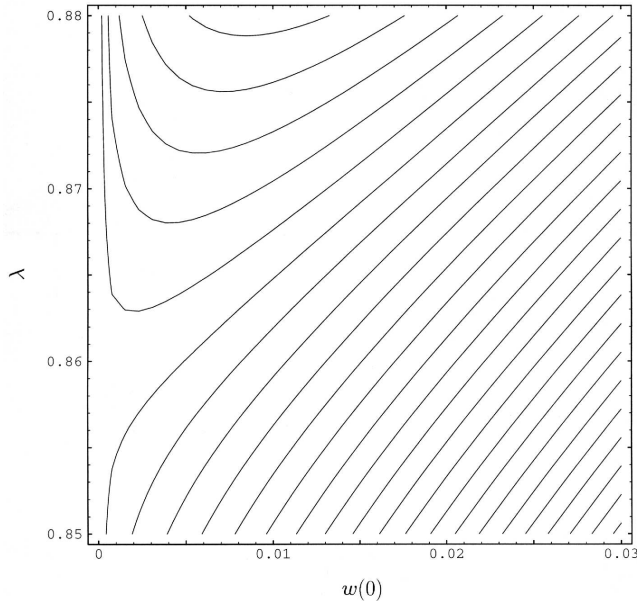


FIG. 4. Contour plot of k^2 for $d = 0.2$ and $\theta^* = \pi/2$ near P_2 . $k^2 = \frac{1}{4}$ along the line $w(0) = 0$. For $\lambda \leq \lambda_2 = 0.858$, k^2 decreases with $w(0)$; for $\lambda > \lambda_2$, k^2 “goes over a hill”.

Fig. 3 shows λ_1 and λ_2 as functions of d for $\theta^* = \pi/2$. The stability domain of the SC state increases monotonically with nonuniformity, following the trend given by the asymptotic formulae (11). Fig. 4 shows a contour plot of k^2 as function of $w(0)$ and λ for $\theta^* = \pi/2$ and $d = 0.2$. This plot looks as if had been copied from that obtained in Ref. 6 for small nonuniformity. For $\lambda < \lambda_2$, k^2 increases monotonically as $w(0)$ decreases; the value $|k| = \frac{1}{2}$ is reached when the order parameter describes the SC state, $w(0) = 0$. On the other hand, for $\lambda > \lambda_2$, the value $|k| = \frac{1}{2}$ is reached while $w(0)$ is still positive; after that, for the minimum of the free energy, k will jump to $-k$ when the magnetic field is swept, so that lower values of $w(0)$ can only be achieved by metastable states.

C. Dependence of $\lambda_{1,2}$ on θ^*

Fig. 5 shows λ_1 and λ_2 as functions of θ^* for $d = 0.1$. The curve for λ_1 has a maximum deviation from $\frac{1}{4}$ for $\theta^* = \pi/2$, and is symmetric about this point. This is qualitatively what one would expect from (11). However, the curve for λ_2 has a marked maximum for $\theta \ll \pi$. This suggests that large domains of stability for the SC state may be found for weak links, provided that the dimensions of the link are properly tuned. The limit $d, \theta^* \ll 1$ will be studied in Sec. III.

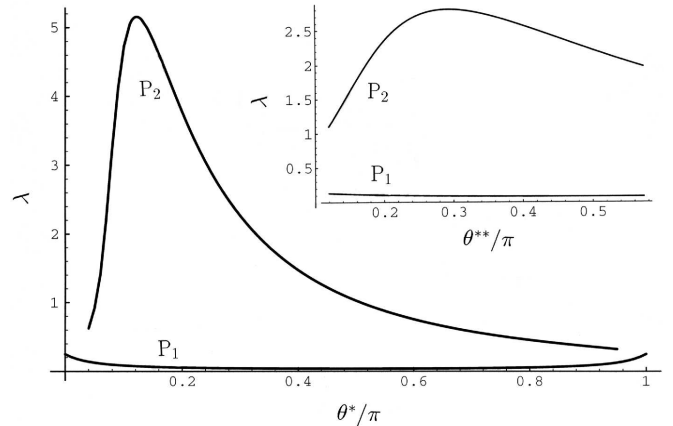


FIG. 5. Position of the critical points as functions of the fraction of the loop where D is small. Here $D(0)/D(\pi) = d = 0.1$. The inset shows these positions for the shape given by Eq. (25), with $p = 2$. Again, $D(0)/D(\pi) \approx d = 0.1$.

D. Location of the Minimum of the Order Parameter

According to Eq. (1), which was derived in Sec. 6 of Ref. 6, the angle where $y(\theta)$ has a minimum and may eventually vanish depends only on the geometry, and not on the temperature or the magnetic field. We want to check whether this result remains true when $D(\theta)$ is far from uniform. The case described by Eq. (12) is not appropriate for this purpose, since the minimum will always be at $\theta = 0$ by symmetry.

As a representative example, we consider a ring formed by three pieces of equal length, with cross sections in the ratio 2 : 10 : 5, as shown in the outer part of Fig. 6. We have calculated $y(\theta; \lambda)$ along the line Γ_{III} (see Fig. 2), where y vanishes for some θ .

The inner part of Fig. 6 shows a polar contour plot of $y(\theta; \lambda)$. The radial coordinate is $\lambda_2 - \lambda$, whereas the angular coordinate is just the angle θ along the ring. For $\lambda = \lambda_1$, $y(\theta)$ vanishes for all θ (outer circumference); for $\lambda > \lambda_1$, $y(\theta; \lambda) = 0$ along the nearly radial line on the upper right. As λ increases, the layer where $y(\theta) = 0$ moves towards the middle of the thin piece of the ring. This could be expected intuitively since, the smaller the coherence length, the less the influence of the neighboring pieces. The arrow at the right shows the angle where the order parameter would vanish according to the asymptotic result (1). We see that the actual result is much less influenced by the neighboring pieces; this tells us that regions where $D(\theta)$ is very small have a stronger influence than what is predicted if only their deviation from the average thickness is taken into account.

We have also evaluated the order parameter along the line Γ_I . As we go from P_1 towards $\lambda = k^2 = 0$, the minimum of the order parameter moves towards the middle of the thin piece, but only by a very small angle.

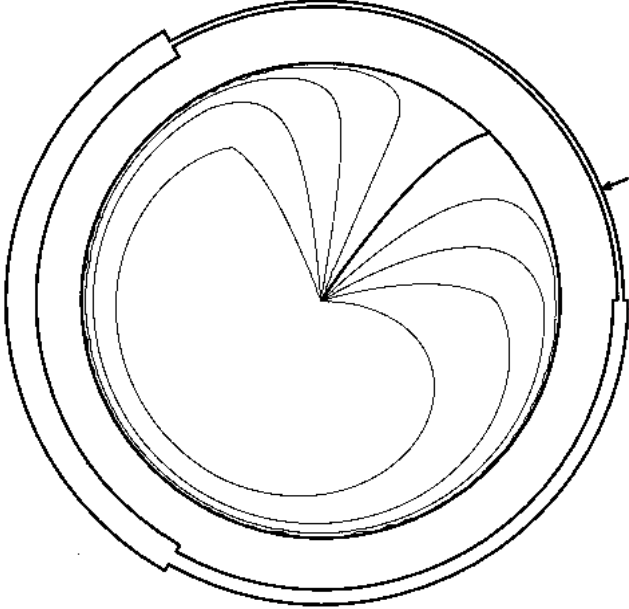


FIG. 6. Outside: an asymmetric loop. Inside: contour plot of the order parameter in this loop for $k^2 = \frac{1}{4}$.

III. WEAK LINKS AND SIMILARITY

We want to evaluate the asymptotic value of λ_2 for $d, \theta^* \ll 1$, near the region where λ_2 is maximum. We shall also assume (and verify a posteriori that this is a self consistent assumption) that $\lambda_2 \gg 1$ and θ^*/d remains finite in this regime. Our initial goal is the evaluation of Λ_R and, for it, we require $w(\theta)$. $w(\theta)$ is obtained from (8), with $w(0) = 1/\Lambda = 0$. Due to the continuity of Dw' , $w'(\theta^{*+}) \ll w'(\theta^{*-})$. This boundary condition, together with $\lambda \gg 1$, make it reasonable to assume $w(\theta) \approx 1$ in the interval $\theta^* \leq \theta \leq \pi$. In the interval $0 \leq \theta \leq \theta^*$ we write $x = \sqrt{\lambda}\theta$, $w(\theta) = \bar{w}(x) = \bar{w}(\sqrt{\lambda}\theta)$, and (8) becomes

$$\bar{w}\bar{w}'' - \frac{1}{2}\bar{w}'^2 + 2\bar{w}^2(1 - \bar{w}) = 0, \quad (18)$$

where the derivatives are with respect to x and the boundary conditions are

$$\bar{w}(0) = 0, \quad \bar{w}(\bar{\theta}) = 1, \quad (19)$$

where $\bar{\theta} = \sqrt{\lambda}\theta^*$. The similarity solution of (18)–(19), $\bar{w}(x)$, is independent of d and depends on λ and θ^* only through the combination $\bar{\theta}$.

By algebraic manipulation, we rewrite (10) as

$$\Lambda_R = 2 \int_0^{\theta^*} \frac{\tilde{f} - f}{f\tilde{f}} d\theta - 2 \int_{\theta^*}^{\infty} \frac{d\theta}{\tilde{f}} + 2 \int_{\theta^*}^{\pi} \frac{d\theta}{f}. \quad (20)$$

Noting that $\tilde{f}(\theta) = \frac{1}{2}d\bar{w}''(0)x^2$, that $f(\theta) = 1$ for $\theta \geq \theta^*$, and changing the variable of integration, this becomes

$$\Lambda_R = \frac{2}{\bar{w}''(0)d\sqrt{\lambda}} \left(\int_0^{\bar{\theta}} \frac{\bar{w}''(0)x^2 - 2\bar{w}(x)}{\bar{w}(x)x^2} dx - \frac{2}{\bar{\theta}} \right) + 2(\pi - \theta^*). \quad (21)$$

At P_2 , $\Lambda_R = 0$. Using (21) and $\theta^* \ll \pi$ we obtain

$$d\sqrt{\lambda_2} = \frac{1}{\pi\bar{w}''(0)} \left(\frac{2}{\bar{\theta}} - \int_0^{\bar{\theta}} \frac{\bar{w}''(0)x^2 - 2\bar{w}(x)}{\bar{w}(x)x^2} dx \right). \quad (22)$$

Eq. (22) gives a universal expression for the scaled $\sqrt{\lambda_2}$ as a function of $\bar{\theta}$ only, for any d which is sufficiently small. Note that $\bar{\theta}$ enters (22) not only through the limits of integration, but also through (19).

The solution of (18) is of the form

$$\bar{w}(x) = \frac{2m}{1+m} \text{sn}^2\left(\frac{x}{\sqrt{1+m}}, m\right), \quad (23)$$

where sn is a Jacobian elliptic function. Given $\bar{\theta}$, m is obtained by numerical solution of (19) and the right hand side of (22) can be evaluated. After $d\sqrt{\lambda_2}$ is known, we also obtain $\theta^*/d = \bar{\theta}/(d\sqrt{\lambda_2})$. In this way we have obtained the universal curve for P_2 in Fig. 7, where $\bar{\theta}$ has been swept as a parameter. We see that λ_2 is of the order of $1/d^2$, provided that θ^*/d is not too small. If this ratio is below $\sim \pi$, the assumption that w almost reaches 1 at $\theta = \theta^*$ is no longer justified.

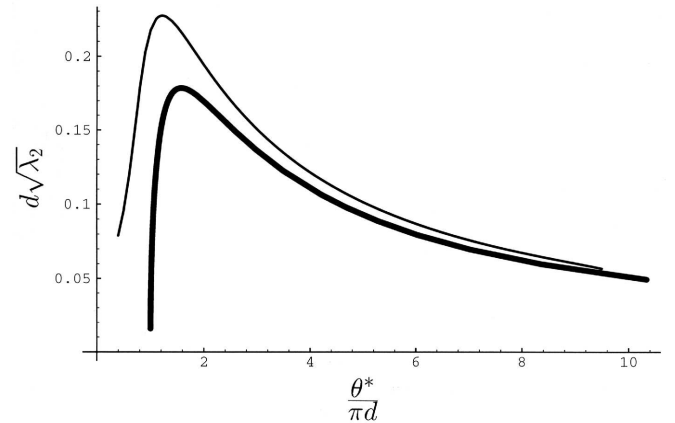


FIG. 7. Position of P_2 for the shape (12) with $d \ll 1$. Thick line: asymptotic line, given by (22); in this case $d\sqrt{\lambda_2}$ depends on θ^*/d only. Thin line: $d = 0.1$.

We are interested in large values of λ_2 . Numerical maximization of (22) gives $d\sqrt{\lambda_2} = 0.179$ at $\bar{\theta} = 0.883$. Denoting by θ_{opt}^* the value of θ^* for which $\lambda_2(d)$ is maximum, this yields $\theta_{\text{opt}}^* = 1.57\pi d$ for $d \ll 1$. On the other hand, (11) gives $\theta_{\text{opt}}^* = \pi/2$ for $d \approx 1$. A simple interpolation formula which has been found to give good results throughout is

$$\frac{\theta_{\text{opt}}^*}{\pi} = \frac{0.734d}{0.468 + d}. \quad (24)$$

We shall close this section by considering the behavior of the loop for “typical experimental conditions” near

the SC state. For given d , we would like $\lambda_2 - \lambda_1$ to be as large as possible; for this purpose, a reasonable choice is $\theta^* = \theta_{\text{opt}}^*$. A typical temperature would be in the middle of the stability domain of the SC state. We therefore define $\lambda_{\text{typ}}(d) = (\lambda_1(\theta_{\text{opt}}^*) + \lambda_2(\theta_{\text{opt}}^*))/2$. Let us now fix $\theta^* = \theta_{\text{opt}}^*$ and $\lambda = \lambda_{\text{typ}}$ and sweep the magnetic flux (which determines k). As a response, the supercurrent $I = k/\Lambda$ varies. It vanishes for $k = 0$ and for $k = \frac{1}{2}$, and reaches its maximum $I = I_{\text{max}}$ for some intermediate value $k = k_{\text{max}}$. In order to characterize the behavior of the loop, we have evaluated $k_{\text{max}}(d)$.

The criterion to determine $k_{\text{max}}(d)$ is as follows. Consider the system of equations that determines ν_i and m_i in Subsec. II.A. Note that k enters these equations only through the constant term in (16) and that this term is an increasing function of I . Therefore, this constant term has a maximum possible value, which is attained at k_{max} . Above this value the system of equations has no solutions and, below it, it has two (one for $k < k_{\text{max}}$ and one for $k > k_{\text{max}}$). At $k = k_{\text{max}}$ the system of equations has a double root and, therefore, its Jacobian vanishes. This provides the additional equation from which $k_{\text{max}}(d)$ can be determined. The results are shown in Fig. 8. Also shown are the values of k at which I has decreased by the factors $\sqrt{2}$ and 2, as the SC state is approached. These are obtained by fixing the constant term in (16).

Fig. 8 shows that the supercurrent decreases sharply as the SC state is approached. This effect might be used for calibration.

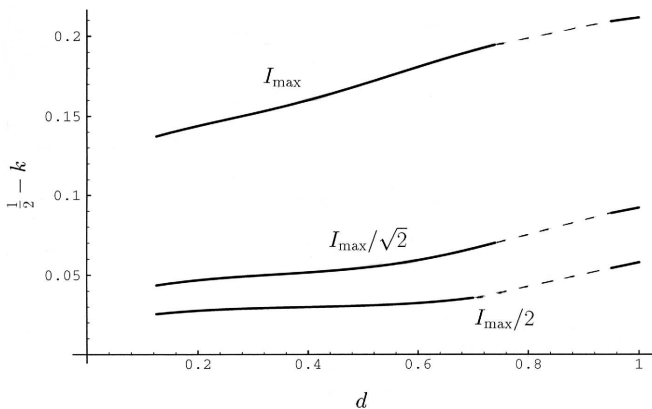


FIG. 8. Rate at which the supercurrent decreases when the SC state is approached under “typical experimental conditions”. Calculations have been performed in the region where m_1 in (13) is complex. For $d \geq 0.95$ we have used the asymptotic results developed in Ref. 6.

IV. DEVIATIONS FROM PIECEWISE CONSTANT THICKNESS

Sections II and III answer our questions for the special case that $D(\theta)$ is of the form (12). We ask now whether the behavior that has been found is typical of loops that resemble a weak link, or arises from spurious features of

the model, such as the discontinuity at $\theta = \theta^*$. For this purpose, we consider D of the form

$$D(\theta) = d + (1 - d) \tanh^p(\theta/\theta^{**}) \quad (25)$$

for $0 \leq \theta \leq \pi$ and symmetric about 0 and π . For $\theta^{**} \ll \pi$ this shape models a weak link with $D(0)/D(\pi) = d$. The larger the value of p , the more the shape of D will resemble a piecewise constant form.

A. Smooth Thickness at $\theta = 0$

We have investigated the case $p = 2$ in Eq. (25). This time the differential equations in (7) or (8) have to be solved numerically. λ_1 is found by linearizing (7), assigning an arbitrary normalization to $y'(0)$, and looking for the smallest value of λ that gives a periodic solution. λ_2 is found by requiring $\Lambda_R = 0$.

In order to evaluate Λ_R , we have to compute $y(\theta)$. For this we solve (7) with the boundary conditions $y(0) = y'(\pi) = 0$. This is still insufficient, since we need the ratio of the strongly vanishing terms $\tilde{f} - f$ and $\tilde{f}f$ near $\theta = 0$. For this purpose, a power series for $y(\theta)$ was developed near $\theta = 0$.

The inset in Fig. 5 shows $\lambda_{1,2}$ as functions of θ^{**} for $d = 0.1$. Fig. 9 is an empirically scaled set of graphs for $\lambda_2(\theta^{**})$. The similarity obtained in Sec. III is no longer obeyed, but the qualitative results of the piecewise constant case are still true: for fixed d , $\lambda_2(\theta^{**})$ has a maximum for some shape of the thickness, $\theta^{**} = \theta_{\text{opt}}^{**}$; as d decreases, the peak of the unscaled $\lambda_2(\theta^{**})$ becomes sharper, with larger $\lambda_2(\theta_{\text{opt}}^{**})$ and smaller θ_{opt}^{**} ; for $\theta^{**} < \theta_{\text{opt}}^{**}$, λ_2 drops sharply.

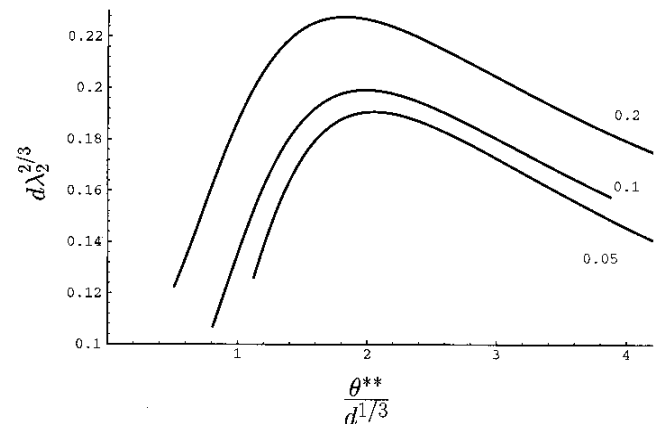


FIG. 9. Position of P_2 for the shape (25), with $p = 2$. The lines are marked by the values of d . The scaling has been chosen empirically to mimic a nearly universal behavior, as in Fig. 7.

B. $D'(0) \neq 0$

We have investigated the case $p = 1$ in Eq. (25), which deviates stronger from piecewise constant than the case $p = 2$. The numerical analysis is very similar to that of the previous section, with one additional subtlety: strictly, the quantity Λ_R defined by (9) and (10) should not be evaluated with the function $w(\theta)$ which describes the SC state. Rather, we should evaluate it with $w(0) > 0$ and take the limit $w(0) \rightarrow 0$. Let us define by $\Lambda_{R,SC}$ the value of Λ_R which is obtained by using the singly-connected order parameter in Eq. (9). Separating Λ_R into a part which is continuous when going to $w(0) \rightarrow 0$ and a remainder, we obtain

$$\lim_{w(0) \rightarrow 0} \Lambda_R = \Lambda_{R,SC} - \frac{D'(0^+) - D'(0^-)}{D(0)^2 w''(0)}. \quad (26)$$

If D is smooth at $\theta = 0$, the last term vanishes.

Using this formula, we have calculated the curves in Fig. 10. As might already be expected, these curves have maxima for suitable θ^{**} , and λ_2 increases when d decreases, but the peaks are less pronounced and the dependence on d is weaker than in the previous examples.

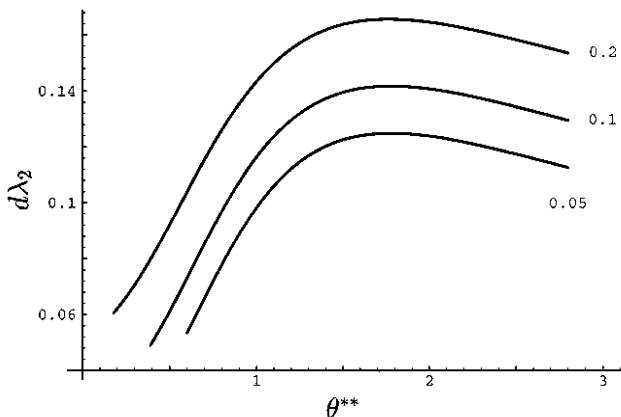


FIG. 10. Like Fig. 9, for $p = 1$.

V. DISCUSSION

The examples considered here extend the results of Ref. 6 to cases where the thickness is far from uniform. The critical points P_1 and P_2 still exist and behave as in Ref. 6. The stability domain of the singly-connected state increases monotonically with nonuniformity. The dependence of λ_1 on θ^* is symmetric about $\pi/2$ and in qualitative agreement with Eq. (11).

There is a surprise in the dependence of λ_2 on θ^* . For the thickness profile defined in (12), $\lambda_2(\theta)$ has a sharp peak when the ring has a “weak link” ($d, \theta^* \ll 1$) and the ratio θ^*/d is appropriately tuned, as found in Sec. III.

In this case, the length of the temperature domain where the SC state is stable is inversely proportional to d^2 .

Modern versions of the Little-Parks experiment are performed on mesoscopic loops, produced by micro lithographic techniques. Smaller values of the perimeter $2\pi R$ allow for smaller values of the coherence length and thus expand the relevant temperature range below T_c . The basic mesoscopic loop is usually repeated a large number of times (e.g. Ref. 11), but there are also cases in which a single loop is used (e.g. Ref. 12). The main contribution of this paper is the design of the thickness profile of the basic mesoscopic ring.

Our goal is to design a sample with a large temperature domain for the SC state. Among the situations considered, we have seen that this is best achieved with the piecewise constant profile (12), with $\theta^* = \theta_{opt}^*$. If θ_{opt}^* is not accurately known, it is safer to take $\theta^* > \theta_{opt}^*$ than $\theta^* < \theta_{opt}^*$. The temperature domain can be increased by decreasing the ratio $d = D(0)/D(\pi)$.

The piecewise constant thickness poses a mathematical problem. Our one dimensional free energy in Eq. (5) is based on the assumption that the order parameter ψ and the supercurrent density vector depend only on θ and remain constant on every given cross section. If $D(\theta)$ is smooth, it has been proven that this assumption is approached when the thickness (linear dimension of D) is much smaller than the perimeter of the loop. But a piecewise constant thickness is not smooth; near the region where the thickness changes, the streamlines are strongly curved and the assumption that the current density remains constant on the cross section is an unrealistic picture. Nevertheless, the results of Sec. IV add confidence to the results of the piecewise constant case as a plausible limit. In order to have a safer answer to the piecewise constant case, and also since the usual experimental situation is that the thickness is smaller than the perimeter only by a moderate ratio, a two dimensional treatment is desirable. Even if the results for the piecewise constant case turned out to stem from an oversimplified free energy functional, the results of Sec. IV indicate that the temperature domain where the SC state is stable increases at least as the ratio $D(\pi)/D(0)$.

It is experimentally possible to make superconductive samples with weak links, such that $D(0)$ is smaller than $D(\pi)$ by several orders of magnitude. However, in this case our theoretical treatment becomes inappropriate. The most important reason is that a large ratio $D(\pi)/D(0)$ implies a large volume where the streamlines are strongly curved and a large influence of the limitation discussed in the previous paragraph. Second, if the coherence length is much smaller than the perimeter, it may not necessarily be much larger than the thickness. And third, far from T_c the Ginzburg-Landau theory is not necessarily a good approximation. Moreover, it is not necessary to have $d \ll 1$; a moderately weak link such as $d \sim 0.1$ will already give a temperature domain which is about twenty times larger than that of the “classic” Little-Parks effect ($0 \leq \lambda \leq \frac{1}{4}$), and should be easily

accessible.

Expression (5) for the free energy neglects the contribution of the magnetic field due to the supercurrent. This contribution was evaluated in Ref. 6 and it enhances the temperature domain for the SC state. This contribution may be important for a large periodic array of rings at $\lambda > \lambda_2$ and $|k| = \frac{1}{2}$; in this case the ground state due to (5) is degenerate and a small perturbation may give rise to collective effects.

Several possibilities for identification of the SC state and the critical point P_2 have been discussed previously.^{3,6} One possibility is to observe directly whether the order parameter vanishes at some layer $\theta = 0$, by means of STM or some decoration technique. Another possibility is to check whether the supercurrent vanishes or jumps for $|k| \approx \frac{1}{2}$; this can be done by means of magnetometer, as in Ref. 13. The SC state was not observed in Ref. 13; conceivably, the effective value of θ^*/d was too low.

For $\lambda > \lambda_2$ and $|k| = \frac{1}{2}$, the free energy is a bistable potential. The potential barrier decreases and the overlap between the order parameters at the minima increases as λ approaches λ_2 . Therefore, fluctuations are expected between both minima, which occur more and more frequently as $\lambda \rightarrow \lambda_2^+$. However, for $\lambda \leq \lambda_2$ the free energy as only one minimum, and no fluctuations are expected. This effect was indeed found in Ref. 14, but it was understood that the sample is in the normal state after the fluctuations disappear. According to the present interpretation, at this stage the sample is in the SC state and is still superconducting. We have seen that P_2 can be pushed to a regime where superconductivity is well developed, so that this bistable potential might open the possibility for low dissipation logical devices.

If P_2 is pushed to a sufficiently low temperature and thermal excitations are rendered unimportant, one may expect to achieve macroscopic quantum coherence¹⁵ of both minima in the bistable potential. This situation was looked for in the past with Josephson junctions.¹⁶ The setup described in this article seems to be cleaner and more promising: there are no uncontrollable parts in the loop, no external current and less sources of dissipation.

To summarize: our results indicate that the temperature region where the singly-connected state exists is not necessarily small, and can be readily found with existent experimental techniques.

ACKNOWLEDGMENTS

This research was supported by the US-Israel Binational Science Foundation. J. B. was also supported by the Israel Science Foundation.

- ² M. Tinkham, *Introduction to Superconductivity*, Krieger, Malabar (1980).
- ³ J. Berger and J. Rubinstein, Phys. Rev. Lett. **75**, 320 (1995).
- ⁴ C. M. Elliott, H. Matano and T. Qi, Euro. J. Appl. Math. **5**, 431 (1994).
- ⁵ E. M. Horane, J. I. Castro, G. C. Buscaglia and A. López, Phys. Rev. B **53**, 9296 (1996).
- ⁶ J. Berger and J. Rubinstein, SIAM J. Appl. Math., in press (available as supr-con/9608001).
- ⁷ J. Rubinstein and M. Schatzman, preprint.
- ⁸ H. J. Fink, A. López and R. Maynard, Phys. Rev. B **26**, 5237 (1982); H. J. Fink, V. Grünfeld and A. López, Phys. Rev. B **35**, 35 (1987); H. J. Fink, J. Loo and S. M. Roberts, Phys. Rev. B **37**, 5050 (1988).
- ⁹ V. V. Moshchalkov, L. Gielen, M. Dhallé, C. Van Haesendonck, and Y. Bruynserade, Nature **361**, 617 (1993).
- ¹⁰ M. Abramowitz and I. A. Stegun, *Handbook of Mathematical Functions*, U.S. Nat. Bureau of Standards (1964).
- ¹¹ P. L. Gammel, P. A. Polakos, C. E. Rice, L. R. Harriott, and D. J. Bishop, Phys. Rev. B **41**, 2593 (1990); A. Bezryadin and B. Pannetier, J. Low Temp. Phys. **98**, 251 (1995).
- ¹² V. V. Moshchalkov, L. Gielen, C. Strunk, R. Jonckheere, X. Qiu, C. Van Haesendonck, and Y. Bruynserade, Nature **373**, 319 (1995).
- ¹³ A. H. Silver and J. E. Zimmerman, Phys. Rev. **157**, 317 (1967).
- ¹⁴ J. E. Lukens and J. M. Goodkind, Phys. Rev. Lett. **20**, 1363 (1968), W. den Boer and R. de Bruyn Ouboter, Physica **98B**, 185 (1980).
- ¹⁵ A.J. Leggett, in *Directions in Condensed Matter Physics*, vol. 1, edited by G. Grinstein and G. Mazenko (World Scientific, Singapore, 1986); A.J. Leggett, in *Chance and Matter*, edited by J. Souletie *et al.* (North-Holland, Amsterdam, 1987).
- ¹⁶ R. J. Prance, J. E. Mutton, H. Prance, T. D. Clark, A. Widom and G. Megaloudis, Helv. Phys. Acta **56**, 789 (1983); M. H. Devoret, J. M. Martinis, D. Esteve and J. Clarke, in *Chance and Matter (ibid.)*

¹ W. A. Little and R.D. Parks, Phys. Rev. Lett. **9**, 9 (1962); R. D. Parks and W. A. Little Phys. Rev. **133**, A97 (1964); R. P. Groff and R. D. Parks, Phys. Rev. **176**, 567 (1968).